2013

Energy controls on diurnal snowmelt events and stream recharge, Lost Horse Canyon, Bitterroot Mountains, MT

Brett Woelber
The University of Montana

ENERGY CONTROLS ON DIURNAL SNOWMELT EVENTS AND STREAM RECHARGE, LOST HORSE CANYON, BITTERROOT MOUNTAINS, MT

By
Brett Woelber
B.A. Geology, Middlebury College, Middlebury, VT, 2010

Thesis

presented in partial fulfillment of the requirements
for the degree of

Master of Science
in Geosciences

The University of Montana
Missoula, MT
Summer 2013

Approved by:

Marco Maneta, Chair
Department of Geosciences

Joel T. Harper
Department of Geosciences

Kelsey Jencso
College of Forestry and Conservation

Woelber, Brett, M.S., May 2013 Geosciences

ENERGY CONTROLS ON DIURNAL SNOWMELT EVENTS AND STREAM RECHARGE, LOST HORSE CANYON, BITTERROOT MOUNTAINS, MT

Chairperson: Marco Maneta

ABSTRACT

Streamflow and groundwater response to snowmelt in forested subalpine catchments carry integrated information about snowmelt events within the basin at different temporal scales. High frequency snowmelt events are often dominated by the day-night cycle, which is reflected in groundwater and streamflow dynamics. Prior studies have highlighted the importance of sub-daily streamflow fluctuations in these catchments for nutrient cycling, riparian aquifer pumping, and surface water availability. In studies that predict stream response to snowmelt or precipitation, sub-daily fluctuations in hillslope water storage are rarely considered as a tool to assess the role of hillslopes in moderating stream recharge from snowmelt runoff over sub-daily timescales. In this study we compare high frequency (15-minute) atmospheric radiation and its influence on the timing and magnitude of both water table and stream stage fluctuations. We analyze net radiation over the snowpack to approximate the energy state of the snowpack and relate it to hillslope hydrologic response and changes in stream stage. Our results suggest that the snowpack cold content must be overcome on a daily basis before recharge to the soil can occur. Until the snowmelt process is resumed, both hillslope water storage and stream stage decrease. We conceptualize the process as a linear series of energy and water reservoirs that fill and deplete driven by the daily atmospheric cycle. By measuring the timing of diurnal peaks in radiation, groundwater response, and stream stage over an entire melt season, we assess the role of the snowpack and hillslopes as filters that moderate and delay the movement of water from the top of the snowpack to local stream systems. Our interpretation of shifts in the timing of diurnal peaks in groundwater and stream stage suggests that once hillslopes become saturated in the uppermost 50 cm of soil, the energy state at the top of the snowpack, the physical properties of the snowpack, and the length of the hillslope that is saturated determine the timing of stream recharge from diurnal snowmelt events. Finally, we present two conceptual models that capture hillslope- and watershed-scale processes that moderate stream recharge during the spring melt season.

PREFACE

Chapter 1 of this thesis, titled “ENERGY CONTROLS ON DIURNAL SNOWMELT EVENTS AND STREAM RECHARGE, LOST HORSE CANYON, BITTERROOT MOUNTAINS, MT”, is written in manuscript form with the intent of submitting it for publication. Consequently, text and figures are written and displayed in an effort to emphasize succinctness and brevity.

ENERGY CONTROLS ON DIURNAL SNOWMELT EVENTS AND STREAM RECHARGE, LOST HORSE CANYON, BITTERROOT MOUNTAINS, MT

1. INTRODUCTION

Accurately predicting snowmelt and streamflow response remains an unsolved problem in the field of hydrology. During the spring, the magnitude of groundwater flow in Rocky Mountain headwater catchments is largely determined by fluxes of snow melt (McNamara et al., 2005). Some research estimates that snowmelt comprises up to 80% of streamflow (Daly et al., 2000). However, very few instrumented sites exist in high mountain areas where the majority of winter snowfall accumulates. Consequently, little is known regarding snowmelt, throughflow, and the resulting stream recharge processes at high elevations. This limits the ability to predict streamflow from snowmelt, especially in first-order streams when streamflow is maintained by high-elevation snowmelt late into the melt season.

Much recent research in the field of runoff generation hydrology focuses on threshold response of watersheds and hillslopes to precipitation events (e.g. Graham et al., 2010; Smith et al., 2010). During a precipitation event, the magnitude of runoff generation in alpine headwater catchments can be predicted by the soil moisture states that evolve over the course of the year (McNamara et al., 2005; Moore et al., 2011; Penna et al., 2011), in addition to the physical properties of catchment soils and hillslope morphology (James and Roulet, 2009). The factors that control the redistribution of soil water and the discharge of water to streams are largely responsible for the observed non-linearity in the streamflow response to precipitation. Soil water storage state is an important variable that can influence the transmission of water and pressure through a hillsope and has been demonstrated in field experiments (Torres, 2002). Results indicate that when soil moisture deficits are low, hillslope transmission increases and runoff generation typically occurs. Bedrock topography (Freer, 2002; Tromp-van-Meerveld and McDonnell, 2006) or some combination of physical properties of a watershed (Hopp and McDonnell, 2009) have also been identified as further controls on the nonlinear hydrologic response of hillslopes and small headwater catchments.

Unlike rain which can occur year-round in events of irregular duration and intensity, snowmelt occurs mostly in the spring forming a multi-month input event whose hourly magnitude varies with the day-night cycle (Flint et al., 2008). The primary difference between studies that examine snowmelt inputs as opposed to precipitation inputs is the regularity of snowmelt inputs to hillslopes during the melt season. This continuous snowmelt input can rapidly overwhelm the soil storage capacity of hillslopes and cause substantial increases in runoff regardless of the bedrock topography or physical characteristics of the hillslope (Smith et al., 2011). In dry snow-dominated watersheds, runoff generation is highly sensitive to soil moisture thresholds. Under highly saturated soil moisture conditions, streamflow initiation and cessation may become more sensitive to snowmelt events (Seyfried et al., 2009). A marked feature of hillslopes during the spring freshet, as opposed to precipitation-controlled seasons, is the duration and magnitude of hillslope saturation. As long as snow is actively melting, meltwater inputs significantly exceed evapotranspiration outputs, augmenting the soil water storage and generating an increasingly connected soil saturated layer at the soil-bedrock interface over the whole-slope (McNamara et al., 2005). In soils underlain by relatively impermeable and unfractured bedrock, percolation at the soil-bedrock interface is often exceeded by infiltration and downslope transmission of snowmelt water during most of the melt season. The pooling of

meltwater at the relatively impervious soil-bedrock interface often promotes the formation of shallow saturated layers and creates lateral transfers of water that can reach streams (Flint et al., 2008).

The idea of saturated layers suggest that the hillslope response to infiltration events is dictated not by the overall soil moisture state over a hillslope, but by the presence of hydrologically active areas across a watershed that are connected to local stream systems (Ocampo et al., 2006; Jencso et al., 2009). The occurrence of rain or snowmelt does not mean that the response of hillslopes is immediate. Because runoff relies on the hydrologic connection of subsurface flow paths, even when hillslopes are in a state of full saturation, hydrologic response may occur with significant delays after an input event. Storm water that is rapidly transmitted to streams often comprises as little as 30% of the overall event runoff (McGuire and McDonnell, 2010), indicating that slower subsurface water transmission mechanisms such as throughflow may dominate hillslope hydrology. This idea of hydrologic connectivity of subsurface flow paths, dynamically evolving to generate the response of a watershed, has been successfully applied to snow-dominated systems (Jencso et al., 2010). The concept of hydrologic connectivity within hillslopes suggests that stream recharge during the spring melt is dictated not by a homogenous response of hillslopes across the watershed, but rather, the hillslopes within the watershed. To better understand the function of connectivity in snow-dominated systems and diurnal stream recharge mechanisms, theories involving snowmelt movement through the subsurface and stream recharge must be better explored over sub-daily time scales.

The study of diurnal cycles of snowmelt, water table, and stream recharge fluctuations in snow-fed river systems complements the study of diurnal streamflow signals in areas dominated by evapo-transpiration (e.g. Wondzell et al., 2010) or glacial melt (e.g. Magnusson et al., 2012). In the early portion of the snowmelt hydrograph, variations in daily temperature and insolation frequently cause snow to melt during the day and refreeze during the night (Fierz et al., 2003). Night-time snowpack refreeze imposes a loss of energy that effectively delays snow melt until heat added during the day exceeds the cold content of the snowpack from the night. This freeze/thaw pattern drives diurnal patterns of snow melt, and has been studied as a mechanism that creates daily additions of water to the hyporheic zone when stream stage is increased and streams are in an influent state (Loheide and Lundquist, 2009). In regions where the direction of recharge is from hillslopes to streams, the diurnal melt signal is reflected in the spring hydrograph by increased stream discharge late in the day following snowmelt, and decreased stream discharge in the early morning once melt has ceased and hillslopes have drained (Lundquist, 2005b).

Diurnal snowmelt processes and their reflection in groundwater levels and streamflow are important for two main reasons. First, it has been shown that diurnal variations in snowmelt cause a daily increase in solute transport and nutrient exports. Worrall et al. (2013) found that the estimation of daily concentration of chemical species needed a correction of up to 25% of the measured value to account for diurnal runoff depending on the time of day when samples were taken. Second, the timing of diurnal peaks in spring streamflow relates to the evolution of basin snowmelt patterns and the characteristics of snow at the watershed scale (Lundquist, 2005a; 2005b).

For a diurnal signal to be present in the stream stage record we first need a diurnal cyclic forcing. Second, this forcing must be transmitted through the hydrologic network from hillslopes to streams. Third, that forcing must arrive as a coherent signal at a stream gauge location (Wondzell et al., 2010). We adapt this framework to snow driven systems by tracing the origin

and movement of diurnal melt signals from the surface of the snowpack to local stream systems. For this we propose that the diurnal signal should be monitored at the surface of the snowpack, through hillslopes, and to stream gauges. The objective of this paper is to extend our knowledge of diurnal snowmelt event response by (1) relating daily groundwater fluctuations to radiative exchanges at the surface of the snowpack, and (2) analyzing how daily groundwater fluctuations caused by snowmelt are propagated to local stream systems.

2. SITE DESCRIPTION AND INSTRUMENTATION

The Lost Horse Canyon (LHC) is a 193 km^2 drainage feeding into the Bitterroot Valley, an important agricultural and recreational area in western Montana (Figure 2). LHC is an E-W trending, glacially-formed, forested canyon in the Bitterroot Mountains of Montana carved from granitic bedrock of the Idaho batholith. The drainage has two Snowpack Telemetry (SNOTEL) sites that measure temperature and the snow water equivalent (SWE) of the snowpack.

Our study site, defined by the total contributing area above the stream gauge, covers a subwatershed with an area of 2.86 km^2 in the upper part of LHC and spans elevations from 1950 to 2250 mASL (Figure 1). It consists of a number of gentle (approximately 14°) north-facing hillslopes and steeper (20° to 25°) south-facing hillslopes. The subwatershed is covered by open areas of grass and shrub vegetation intermixed with stands of Douglas fir (Pseudotsuga menziesii), sub-Alpine fir (Abies lasiocarpa) and Englemann spruce (Picea engelmannii). Bedrock in this area is overlain by sandy to silty-loam soil as per the USDA textural classification system. At this site and in other areas in the sub-catchment, the depth to which soil can be excavated is roughly 50 cm. Geophysical methods reveal a 30 cm layer of saprolite under this soil layer and above un-weathered granite bedrock. The watershed is drained by a first-order perennial creek with a ~10 meter wide riparian zone. Annual precipitation at this elevation in LHC varies from 50 to 70 inches per year, the majority of which falls in the form of snow. Snow cover begins in late October, and persists to late June.

A 40 m long, north-facing hillslope at the bottom of this subwatershed was instrumented with a meteorological station and shallow monitoring wells (Figure 1). The meteorological station is equipped with the following instruments: air temperature and relative air humidity (Campbell Scientific HMP 50), barometric pressure (Campbell Scientific CS106), precipitation (Campbell Scientific TE525), snow depth (Campbell Scientific SR50A), wind velocity and direction (Campbell Scientific RM Young 05103-45), net radiation (Campbell Scientific NR-LITE), and incoming and reflected shortwave radiation (Campbell Scientific CS300). These sensors were positioned at a height of 4 meters above the ground surface to remain above the snow surface. Atmospheric data from this station were recorded at 15-minute intervals. Snow water equivalent (SWE) was taken from the Twin Lakes snowpack telemetry (SNOTEL) station located ~100 meters from the study site.

Five wells were placed in the anticipated path of groundwater flow along the study hillslope. These wells were placed with a drive-point rod and sleeve, pounded to the point of refusal, and installed with 0.5 inch PVC. Wells were backfilled with sand and capped with bentonite. These five wells were instrumented with HOBO pressure transducers (error +/- .3 cm), which continuously measured water table height at 15 minute intervals. Water table height recorded by these pressure transducers was calibrated with manual measurements of well water depth in the field. Saturated hydraulic conductivity (K_{sat}) was estimated with both lab and field techniques. Eight field measurements of saturated hydraulic conductivity were taken using a

Guelph permeameter at variable depths (15, 30, and 45 cm). Lab-based measurements of K_{sat} (n=18) were measured with a falling head permeameter on horizontally- and vertically-cored soil samples collected at 15, 30, and 45 cm. Soil porosity measurements were estimated with saturation tests (n=11) and corroborated with measurements of soil volumetric water content while under conditions of full saturation.

Stream stage was monitored in the perennial stream at the research site. The in-stream transducer was placed in a pool reach. Stage was computed by subtracting measurements of barometric pressure from the measurement of pressure taken by each underwater transducer (e.g. Loheide and Lundquist, 2009). These measurements were calibrated with manual measurements of stream stage taken in the field.

50 megahertz (MHz) ground penetrating radar (GPR) was used to characterize the subsurface in and around the research location. Transects were run in straight lines across the research site in areas where the absence of downed trees and uneven terrain would reduce acquisition errors. The start and end locations of these transects were recorded with a Leica TS06 total station to georeference GPR transects. We estimated mean constant velocity of the material by fitting diffraction hyperbolae to a number of point source diffractors. Mean constant velocity was then used to quantify the distance from surface to bedrock along each of eleven straight transects. The total station was used to survey the study site and surrounding area at ~1m resolution.

3. DATA ANALYSIS METHODS

Net radiation, well, and stream time-series data were processed using a soft low-pass filter to reduce high frequency noise while preserving the timing of daily maxima. The filtering process permitted a better identification of the diurnal maximum of net radiation, groundwater, and streamflow. In this paper we define R_{peak} as the timing of the peak of net radiation measured in minutes from midnight. Similarly, we define GW_{peak} as the timing of maximum response in wells (maximum pressure head) measured in minutes from midnight. Finally, we define S_{peak} as the timing of maximum stream stage measured in minutes from midnight (Figure 2). The timing of R_{peak} was manually identified and recorded for each day, while GW_{peak} and S_{peak} were also manually identified but only recorded for days when the peaks exceeded the local average by an amount larger the combined errors from pressure transducers inside and outside the wells (0.6 cm).

To study the response time between energy inputs at the top of the snowpack and the hydrologic response of the hillslope and the stream we analyzed the time elapsed between maximum daily net radiation (R_{peak}) -which is assumed to represent the moment when accumulated radiative energy to the snowpack was at a maximum- and the moment when soil recharge was at its maximum (GW_{peak}). We plotted the difference between R_{peak} and GW_{peak} over time to study the hydrologic response of the soil to the daily energy cycle changes as the melt season advanced. Similarly we plotted the difference between GW_{peak} to S_{peak} over time to study the hillslope-to-stream hydrologic dynamics.

To understand the effect of nighttime radiation losses from the snowpack in the daily snowmelt cycle, we further define δ as the time, in minutes, required for daytime positive net radiation inputs to recover the energy lost from the snowpack due to outgoing nighttime radiation. Quantity δ, which we term "daily replenishing time" was calculated every day of the

melt season and provides an estimate of the cold content inertia that needs to be overcome daily before melt can resume.

4. RESULTS

4.1 Hydrostratigraphy and K_{sat}

Eleven GPR transects were used to characterize the study site, three of which are displayed (Figure 3). The interface between regolith and bedrock, indicated by the dashed red line in the figure, can be interpreted as the strong return at 80-90cm. The depth to bedrock does not vary appreciably among transects, and ranges from 80 to 90 cm (error +/- 10 cm.). Soil pits dug around the study site encounter regolith at approximately 50 cm. With this information, we characterize the hydrostratigraphic layers in the study site as 50 cm of mineral soil (blue dash line in Figure 3) overlying 30 to 40 cm of regolith. Soil depth data during the installation of wells support the GPR estimates of soil depth. Four wells in the study hillslope exceed 30 cm in depth, and one well exceeds 50 cm in depth.

A visual examination of GPR transects at the study site show undulations in the strong return that signifies bedrock in the study area. These undulations could be a result of non-planar bedrock topography but could also be the result of acquisition errors from operating a GPR unit in an uneven surface terrain and of large rocks and boulders embedded in the soil matrix. Both blue and red lines are dashed to represent the uncertainty of the depth and shapes of the soil-regolith and regolith-bedrock boundaries.

The analysis of K_{sat} measurements show no significant differences between values calculated from the Guelph permeameter in-situ test and falling head permeameter lab tests, or at different depths or orientations (Table 1). Because of this, we consider the soil to be isotropic and homogenous. Below the uppermost 50 cm of mineral soil is 30 cm of weathered bedrock, and below that solid bedrock. An average value for K_{sat} was calculated to be 1.5 meters/day for all measurements in the upper 50 cm, 0.0864 meters/day for weathered granitic bedrock (Kosugi et al., 2006), and 0.0864 meters/day to 8.64×10^{-8} meters/day for unweathered granite bedrock (Martinez-Landa and Carrera, 2005). Saturation tests of the upper 50 centimeters of mineral soil yield a porosity of 0.52, which is similar for saprolite. The water storing capacity of mineral soil and saprolite in the area is identical, however, given a slightly greater thickness of mineral soil and ten times the K_{sat} of underlying saprolite, we consider the uppermost 50 cm of mineral soil the main water transmitting hydrostratigraphic unit in this study.

4.2 Radiation and Snowmelt Response

The time series data for net radiation, snow water equivalent (SWE), groundwater, and stream stage for the entire study period is presented in Figure 4, which spans the time from the maximum SWE peak, as measured by the nearby Twin Lakes SNOTEL station, to the cessation of well response. Net radiation illustrates the diurnal radiative cycle, with positive radiation balances into the snowpack during daytime controlled by incoming solar radiation to the snowpack, and negative radiation balance during the night, when long wave radiation emissions from the snowpack dominate. We assume that during the melt season most of the snowpack is isothermal except the top of the snowpack exposed to atmospheric and radiative fluctuations. During the study period, three distinct multi-day storms occurred, one in early May, one in late

May, and one in early June (Figure 4). During these multi-day storms, there are relatively small-magnitude and shorter-duration positive radiation inputs to the snowpack during the day due to cloud cover and relatively high negative radiation outputs from the snowpack during the night. During these multi-day storms, rain on snow events or snow accumulation events may have also occurred.

Snow water equivalent decreases monotonically but at variable rates during the spring melt (Figure 4). Ablation rates are up to three cm/day early in the melt season and up to seven cm/day late in the melt season as days grow longer. During multi-day storms, daily snowmelt ceases to occur and SWE remains constant for five-day periods or increases during precipitation events. During these multi-day storms, the cessation of snowmelt corresponds with a disappearance of the diurnal signal in both the water table as well as in the local stream network (Figure 4).

4.3 Diurnal response of GW and Stream

The daily response of wells to melt inputs varies according to their position in the hillslope, but the seasonal response of all wells exhibits a similar pattern over time. The effect of multi-day storms and the associated reduction in snowmelt is clearly reflected in the significant drawdowns in early and late May as well as early June. A close look at the well response indicates that some wells (e.g. well 3) are less sensitive to the daily diurnal signals while others (e.g. well 4) are highly responsive to daily melt events. No clear connection of the responsiveness of wells to each daily snowmelt event with respect to their position lower or higher on the study hillslope was detected.

Seasonal trends observed in all wells can be divided into three distinct groundwater periods. April 20 to May 10 is characterized by transient responses to radiative forcing. Wells fully saturate and fully draw down during this 20 day period in response to melt and refreeze events. Fluctuations in the soil saturated layer during this early transient period are between 10 and 25 centimeters among all wells. During this time, groundwater levels at wells located uphill show a greater drawdown, with well 1 drawing down in excess of 25 cm. The fluctuations were progressively dampened at well locations down the slope, with well 5 drawing down less than 10 cm. From May 10 to June 25, the hillslope was under conditions of full saturation and fluctuations in the water table between days were rarely greater than three centimeters. From June 25 to July 10, the well levels receded in response to snowpack disappearance and a cessation of snowmelt inputs to the hillslope. Uphill well water levels decreased sooner and at a faster rate than downhill wells (Figure 4). The diurnal response of ground water levels to small or large radiation events was relatively fast. In all cases it occurred on the same day as the radiation event. Similarly, the diurnal response of stream stage to changes in the level of soil saturation occurred on the same day as the change in the level of soil saturation. During multi-day storms, stream stage decreased and the presence of diurnal fluctuations disappeared or was heavily dampened. During melt events, stream stage increased and the presence of diurnal fluctuations resumed or was amplified.

The timing of peak well response (GW_{peak}) consistently lagged the timing of maximum net radiation (R_{peak}), and the timing of daily maximum stream stage (S_{peak}) consistently lagged GW_{peak}. Figure 5 shows the size of such offset between R_{peak} and GW_{peak} over time for the five wells. As the melt season progressed, the lag between R_{peak} and GW_{peak} decreased in all wells indicating a faster response of wells during each progressive day of the spring melt. In order to

capture seasonal melt dynamics this trend was fit with a linear trend line, which maximizes the R^2 values while also maximizing the randomness of the fitted residuals. Well 3 has the smallest daily decrease in response time (-0.22 min/day), while well 4 exhibited the largest decrease in response time as the melt season advanced (-10.32 min/day). Significance statistics of the trends using the Kendall-Mann trend test and a trend test for linear regressions are presented in Table 2.

While the decrease of response time between R_{peak} and GW_{peak} show a somewhat linear trend, the seasonal change in response time between GW_{peak} and S_{peak} show a nonlinear parabolic trajectory (Figure 6). Fitting a quadratic trend line to this dataset maximizes the R^2 values of these parabolic trends while maximizing the randomness of the fitted residuals. Early in the melt season, GW_{peak} and S_{peak} occur almost simultaneously. As the melt season advances, well response precedes stream response by up to 500 minutes indicating that the contributing area to the stream has increased and extended to regions further away from the stream with longer travel times. Late in the melt season, GW_{peak} and S_{peak} are again temporally coincident indicating that the contributing area has shrunk back to a smaller region close to the stream. Well five lacked enough discernible diurnal maxima for a meaningful nonlinear trend to be applied.

The time taken every morning to overcome the energy lost to long wave emission from the snowpack is shown in Figure 7. As the nights grew shorter, the time it takes to overcome the energy hurdle produced by the nighttime losses and to resume the daily snowmelt cycle shrinks on average by 0.75 min, although there is high variability due to atmospheric conditions, especially early in the melt season when cloudy days were more frequent. The trend presented in Figure 8 is statistically significant (Kendall-Mann trend test P-value=0.023; simple linear regression trend test, P-value=0.0964). The total time needed to overcome the energy hurdle ranged from 200 minutes in mid-April to 100 minutes in early July. Given the relatively short days in April, a delay of more than 3 hours takes a significant time of the effective daily melting period. During each of three multi-day storms observed during the 2012 melt season, the role of daily replenishing time (δ) in delaying melt at the snow surface can be further illustrated. During these colder time periods, negative radiative outputs during the night were not exceeded by positive radiative inputs during the day and snowmelt did not resume. During these periods SWE levels did not change, well levels declined, and stream stage decreased.

5. DISCUSSION

5.1 What role do fluxes of radiation play in snow dominated systems?

The consistent offset between R_{peak}, GW_{peak} and S_{peak} is an indication of causality between energy, hillslope, and stream response. Stream recharge from diurnal melt events had a prompt, same-day response to radiative forcing indicating a strong atmosphere-snowpack-soil-stream hydraulic connection very sensitive to the day-night energy exchanges at the top of the snowpack. We argue that daily radiative exchange at the snowpack surface is a good proxy for predicting fluctuations in the water table, which in turn determine changes in local stream stage. An important consideration made in this paper is that turbulent energy exchanges (i.e. latent and sensible heat) between the snowpack and the lower atmosphere in semi-alpine environments are of secondary importance to radiative exchanges. This consideration is based on the idea that in snow-dominated, high-elevation systems radiation is a strong predictor of snow water equivalent (SWE) on different aspects (Elder et al., 1991). Moreover, in forested snow-covered areas, measurements of net radiation capture energy dynamics created by the shading of shortwave

radiation by canopies and re-radiation of longwave radiation unique to forested areas (Pomeroy et al., 2009). In the study location, wind speeds rarely exceed 2 m/s and are usually lower, providing small forcing for turbulent exchanges. Net radiation is also highly correlated with the air temperature cycle over sub-daily time scales and therefore includes a large share of the information contained in the air temperature record. During each of three multi-day storms captured in our study period, high values of nightly negative net radiation are reflected in sub-freezing night-time temperatures. At all other points in the melt season, low values of nightly negative net radiation correspond to above-freezing nights.

Another important consideration is that net radiation measures the difference between incoming and outgoing radiation at the surface of the snowpack but does not convey information on the energy state of the interior of the snowpack. Net radiation data does not provide any insight into the thickness, porosity, saturation percent, or hydraulic conductivity of the snowpack either. These factors affect the residence time of melt water in the snowpack, and thus the snowmelt signal travel time from the peak in radiation to the peak in groundwater response. In modeling studies that assume the snowpack to be isothermal during the spring melt (e.g. Lundquist, 2005a), important processes that delay the initiation of snowmelt are not represented. Measurements of net radiation clearly show that the snowpack undergoes a day-night energy cycle during which the direction of net radiation flux becomes negative (outgoing) at night (Figure 4). This indicates that over the course of each diurnal cycle, the snowpack likely moves from an isothermal to non-isothermal state if the radiative losses are not compensated by sensible or latent heat inputs. As each day resumes, the snowpack must be brought back to an isothermal state before snowmelt output can be produced (Figure 7).

In general, the daily replenishing time (δ) values decreased linearly over the course of the melt season (Figure 7). Until the summer solstice, nights become both shorter and warmer. After the summer solstice, nights become longer and warmer. In general, during the spring melt the time it takes to input more positive radiation into the snowpack than was lost during the night decreases. This suggests that the snowpack is an energy sink which must be replenished on a daily basis before melt can be resumed. This agrees with radiative energy studies previously conducted in non-forested, snow-covered landscapes (Munneke et al., 2009). The general decrease in δ values over the melt season suggests that the role of nightly snow refreeze has a decreased influence later in the melt season. However, even on the final day of snowmelt, it takes an excess of 100 minutes for positive values of net radiation during the day to exceed radiation lost from the snowpack during the night. Therefore, the day-night radiative balance is a strong control on hydrologic recharge to the subsurface over the course of the melt season.

5.2 What is the relationship between daily snowmelt and groundwater response?

Over the entire melt season, groundwater fluctuations consistently lagged radiative forcing (Figure 5). As the melt season progressed, the difference between R_{peak} and GW_{peak} in all five wells decreased linearly (Figure 5). Even though only well 4 shows a significant trend at a high level of confidence, the fact that all the trends are consistently negative lends reasonable assurance that the analysis is not just a product of chance but that it captures actual hillslope processes in which well response time to diurnal snowmelt events decreases over time. Multiple processes could reduce the time it takes for a peak in radiative inputs to translate to a peak in groundwater. First, the amount of time it takes each day to bring a snowpack to an isothermal state varies. Second, changes in snowpack thickness and saturation determine how quickly water

moves from the top of the snowpack to the base. And third, the thickness and saturation state of the vadose zone determines how quickly melt water at the base of the snowpack percolates vertically to the water table. In the sub-Alpine hillslope instrumented for this study, the vadose zone is minimal or non-existent during the spring melt when hillslopes are mostly or entirely saturated. Therefore, we interpret the gradual reduction in the delay from R_{peak} to GW_{peak} over the melt season also as an indication of gradual snowpack thinning. This agrees with prior research involving diurnal snowmelt timing at different basin scales (Lundquist, 2005b).

From April 25 to July 10, the presence of water in all wells at the research site indicates that water was being transmitted through the highly conductive uppermost 50 cm of mineral soil of the hillslope. While the uppermost 50 cm of soil are saturated, three distinct hillslope behaviors were observed (Figure 3). In these three periods, similar net radiation forcing produced different groundwater response. During the first period, from April 20 to May 10, small net radiation events create large changes in groundwater levels. During the second period, May 10 to June 25, large amplitude net radiation cycles generate small changes in observed groundwater levels. The third period from June 25 to July 10 is defined by a slow decrease of groundwater levels associated with the snowpack melt-out in the hillslope. The drawdown in downslope well positions is partially compensated (more sustained) by water contributions from uphill sources. In the first two periods the effect of multi-day storms are apparent. In early May, a multi-day storm creates groundwater drawdowns of 10 to 25 cm. In late May, a multi-day storm creates only three to five cm. drawdowns in all five wells. We attribute the differences in response to the different antecedent wetness conditions across the hillslope during each of these distinct periods. Period one is characterized by low antecedent wetness conditions where small reductions in snowmelt inputs have a large effect on groundwater levels because there still are large potential gradients in the soil and large amount of space available to redistribute soil water. The second period is associated with high wetness and snowmelt inputs triggered by changes in net radiation have a small relative effect on a fully saturated soil. Overland flow, which would occur at the base of the snowpack, is also likely during this period. Period three is a recession stage where snowmelt inputs cease and water storage in the soil progressively decreases.

Well response over the study hillslope is a function of both local (e.g. snowmelt over the well and specific local properties of the soil) and uphill effects (e.g. lateral inflows). The lateral effects are clear during the recession period described above. Wells downhill had progressively longer and gentler recessions due to uphill areas contributing lateral inflows. The magnitude of daily groundwater fluctuations is also different from well to well. Wells 2 and 4 are highly responsive to the diurnal forcing and show large fluctuations in the water table at a point each day, while the response of wells one, three, and five is muted. We attribute this variation in response to the idiosyncratic properties of the location where these wells were placed. Snowpack heterogeneity (Lundquist, 2005a), changing melt pathways within the snowpack (Albert et al., 1999), hydraulic conductivity of different soil types (Lowry et al., 2010), and macropore flow in the soil (Newman et al., 2004) could all contribute to the daily variations in the magnitude of response seen among wells.

Figure 8 offers a conceptual diagram of the dynamics of the shallow saturated layer in the hillslope that is consistent with the observed behavior of our wells and the existence of the three periods described above. In this conceptual model the position of the water table forms a saturated wedge whose size changes over the course of the melt season (Kendall et al., 1999). During the early phase of the melt season, wells in positions where the saturated wedge is deeper show more moderate drawdowns during snowmelt shutdown events. From May 1 to May 5, a

multi-day storm with low daily radiative inputs and caused a significant drawdown in all wells but the magnitude was higher for uphill wells than for downhill wells. In the downhill positions the saturated wedge is thicker, and a cessation in snowmelt inputs to the hillslope at these locations are moderated by lateral inflows from uphill. During the middle of the melt season, the shallow edge of the saturated wedge is located at some point above the study hillslope and all wells are at a position of full saturation. At the end of the melt season, drawdown occurs sooner and is more rapid for uphill wells than downhill wells, signaling the movement of the saturated wedge downslope. These observations and conceptual model agree with prior studies (e.g. McGuire and McDonnell, 2010) that relate an increase in dissolved solute transport to the extent of hillslope saturation that changes during input events.

5.3 What is the relationship between groundwater and stream recharge?

To assess the role of hillslopes in moderating stream recharge from snowmelt inputs, we calculate the difference in the timing of GW_{peak} and S_{peak} for each day of the melt season and for each well. Differencing the timing of GW_{peak} and S_{peak} provides a measure of the transit time of the diurnal melt signal through hillslopes and provides a means to assess the role of hillslopes in moderating stream recharge from snowmelt inputs. In our study location groundwater level fluctuations rarely lag stream fluctuations, which seems to be a frequent case in alpine meadows (Lowry, 2010) and in till fields bordering glacial outlet rivers (Magnusson et al., 2012) where streams force changes in ground water levels. Instead, stream response generally lags groundwater response with a lag that varies from zero to 500 minutes during the spring melt (Figure 6). Similar results have been found in Nevada watersheds, where seasonal drainage of snowmelt-dominated streams alters hillslope-stream interactions (Huntington and Niswonger, 2012). Over the entire spring melt period, the trend in the lag times from GW_{peak} to S_{peak} is generally parabolic, and reflects the hillslope saturation dynamics that evolve during the course of the spring melt (Figure 8). Early in the melt season, saturation occurs near the hillslope base adjacent to the stream. As the melt season progresses, the extent of the saturated region actively contributing to streamflow moves upslope. Toward the end of the melt season, the extent of saturation is again reduced to near-stream areas.

While overland flow almost certainly occurs each day of the melt season, the timing of maximum groundwater levels is still an important daily measurement that can be used to understand the role of hillslopes. Some wells respond on a daily basis while others only respond some days, suggesting that some landscape positions receive and store daily inputs of meltwater while others remain at saturation over multiple days and immediately transmit meltwater in the form of overland flow. Moreover, overland flow can re-infiltrate into an unsaturated place on the landscape. In addition to different melt pathways through the snowpack, the amount of time it takes specific landscape positions to saturate will change the timing of GW_{peak} for each well. The shape of the daily peak in groundwater level may have some relationship with this exceedance of hillslope water storage capacity. The steeper rising limb of the daily peak in groundwater levels compared with the falling limb may mean that water storage in shallow hillslopes is overwhelmed quickly but drains slowly.

The difference in the timing of GW_{peak} and S_{peak} is a measure of the travel time of the daily melt signal from a hillslope to a stream, and reflects the extent of saturation of the hillslope that contributes throughflow to the stream. To account for the fact that the stream signal detected at the stream gauge is a convolution of all contributing hillslopes, our study was conducted in a

small sub-watershed that spans a small range of elevations and aspects. Early in the melt season, the synchronous timing of GW_{peak} and S_{peak} corresponds to a time when the hillslope saturation extent is small, hillslope transmission of meltwater to streams is fast due to proximity, and hillslopes do little to delay the diurnal snowmelt signal to local streams. During the middle of the melt season, the asynchronous timing of GW_{peak} and S_{peak} corresponds to a time when the hillslope saturated area expands. In this situation hillslope transmission of upslope meltwater to streams is slower due to the increased throughflow travel times that result from increasing distance of the contributing upslope areas. However, melt that occurs on saturated sections of the hillslope may move rapidly as overland flow to the stream. Overall, on this particular hillslope, the delay in the diurnal snowmelt signal increases up to 500 minutes during this period. At the end of the melt season, the timing of GW_{peak} and S_{peak} becomes synchronous again. The cessation of snowmelt inputs after the melt out reduces the size of the saturated wedge. At the minimum size, hillslope transmission of water to streams is almost immediate, with little impact in the delay of the diurnal snowmelt signal to the stream. The role of hillslopes in the transmission of the diurnal energy signal to streams depends on the magnitude of saturated hillslope areas, which expand and then contract over the course of the melt season.

5.4 Implications

The diurnal signals described in this study may be used as a diagnostic tool to assess and monitor the impacts of climate change on high-elevation snow dominated catchments. Catchments such as these are excellent locations to detect change due to their high sensitivity to climate variation. The changes that are most likely under projected climate scenarios in the Pacific Northwest are less precipitation falling as snow (thinning of the snowpack) and warmer temperatures (Abatzoglou, 2011; Burger et al., 2011). The earth is expected to continue rotating at the same speed, so day-night cycles will stay invariable. A dampening or distortion of the diurnal signals in streams may indicate that turbulent energy exchanges (sensible and latent heat) between the snowpack and the atmosphere are starting to dominate snowmelt cycles at high elevation. Similarly, alterations in the relative duration of the snow accumulation and ablation season and in the size of the snowpack may also be detected in the drift of lag times between groundwater and stream response. Potentially smaller snow years would show a hillslope behavior with the same three periods outlined in section 6.2 but with a shortened period of full saturation (period 2) and a tighter parabolic trajectory of the lag time between GW_{peak} and S_{peak} during the melt season. A number of valuable diagnostics at different scales based on streamflow diurnal signals measured at the USGS network of stream gauges have been proposed by Lundquist (2005b). The work presented here shows that diagnostics based on diurnal peaks in stream stage could be used in conjunction with measurements of groundwater dynamics in semialpine catchments for improved detection of climate change.

6. SUMMARY AND CONCLUSIONS

Stream recharge from daily snowmelt events is a complicated process that varies spatially at the watershed scale and temporally over the course of the melt season. This study monitors a hillslope with homogeneous aspect and soil characteristics during the 2011-2012 melt season to study the transmission of the diurnal radiation cycle through the snow-hillslope-stream continuum. Our results suggest that the timing of the diurnal signal found in streams is a function of daily radiative exchanges at the top of the snowpack, movement of melt-water through the

snowpack, and hillslope saturation extent. While net radiation comprises just one portion of the snow surface energy balance, our results suggest that radiative exchange at the snow surface is a good proxy for sub-daily and multi-day snowmelt over the spring melt season.

Over multi-day time scales, multi-day storms can cause an entire cessation of diurnal cycles in snowmelt and lead to drawdowns in the saturation of hillslopes and in stream stage. At our site, hillslope saturation was influenced by the formation and upslope movement of a saturated wedge of water at the soil-bedrock interface. An analysis of the timings between diurnal peaks in well response and peaks in stream stage provides information about the dynamics of the hillslope contributing areas to streams over the spring melt season. Results from this study show that the role of hillslopes in delaying the daily recharge of streams during the spring melt depends on the magnitude of saturated hillslope area under the melting snowpack, which is sensitive to the daily energy cycle. Because of this we suggest that the diurnal signal found in snow-dominated systems may be a valuable diagnostic tool to detect environmental change and to understand the variability of stream recharge at daily timescales.

REFERENCES

Abatzoglou, J. T. (2011). Influence of the PNA on declining mountain snowpack in the Western United States. *International Journal of Climatology*, *31*(8), 1135–1142. doi:10.1002/joc.2137

Albert, M., Koh, G. and Perron, F. (1999), Radar investigations of melt pathways in a natural snowpack. Hydrol. Process., 13: 2991–3000. doi: 10.1002/(SICI)1099-1085(19991230)13:18<2991::AID-HYP10>3.0.CO;2-5

Bürger, G., Schulla, J., & Werner, a. T. (2011). Estimates of future flow, including extremes, of the Columbia River headwaters. *Water Resources Research*, *47*(10), 1–18. doi:10.1029/2010WR009716

Daly, S. F., Davis, R., Ochs, E., & Pangburn, T. (2000). An approach to spatially distributed snow modelling of the Sacramento and San Joaquin basins, California, *3271*(September), 3257–3271.

Elder, K., Dozier, J., & Michaelsen, J. (1991). Snow accumulation and distribution in an Alpine Watershed. *Water Resources Research*, *27*(7), 1541–1552. doi:10.1029/91WR00506

Fierz, C., Riber, P., Adams, E. ., Curran, a. ., Föhn, P. M. ., Lehning, M., & Plüss, C. (2003). Evaluation of snow-surface energy balance models in alpine terrain. *Journal of Hydrology*, *282*(1-4), 76–94. doi:10.1016/S0022-1694(03)00255-5

Flint, A. L., Flint, L. E., & Dettinger, M. D. (2008). Modeling Soil Moisture Processes and Recharge under a Melting Snowpack. *Vadose Zone Journal*, *7*(1), 350. doi:10.2136/vzj2006.0135

Freer, J. (2002). The role of bedrock topography on subsurface storm flow. *Water Resources Research*, *38*(12). doi:10.1029/2001WR000872

Graham, C. B., Woods, R. a., & McDonnell, J. J. (2010). Hillslope threshold response to rainfall: (1) A field based forensic approach. *Journal of Hydrology*, *393*(1-2), 65–76. doi:10.1016/j.jhydrol.2009.12.015

Hopp, L., & McDonnell, J. J. (2009). Connectivity at the hillslope scale: Identifying interactions between storm size, bedrock permeability, slope angle and soil depth. *Journal of Hydrology*, *376*(3-4), 378–391. doi:10.1016/j.jhydrol.2009.07.047

Huntington, J. L., & Niswonger, R. G. (2012). Role of surface-water and groundwater interactions on projected summertime streamflow in snow dominated regions: An integrated modeling approach. *Water Resources Research*, *48*(11), n/a–n/a. doi:10.1029/2012WR012319

James, a. L., & Roulet, N. T. (2009). Antecedent moisture conditions and catchment morphology as controls on spatial patterns of runoff generation in small forest catchments. *Journal of Hydrology*, *377*(3-4), 351–366. doi:10.1016/j.jhydrol.2009.08.039

Jencso, K. G., B. L. McGlynn, M. N. Gooseff, S. M. Wondzell, K. E. Bencala, and L. A. Marshall (2009), Hydrologic connectivity between landscapes and streams: Transferring reach- and plot-scale understanding to the catchment scale, *Water Resources Research*,45, W04428, doi:10.1029/2008WR007225.

Jencso, K. G., McGlynn, B. L., Gooseff, M. N., Bencala, K. E., & Wondzell, S. M. (2010). Hillslope hydrologic connectivity controls riparian groundwater turnover: Implications of catchment structure for riparian buffering and stream water sources. *Water Resources Research*, *46*(10), 1–18. doi:10.1029/2009WR008818

Kendall, K.A., Shanley, J.B., McDonnell, J.J. (1999). A hydrometric and geochemical approach to test the transmissivity feedback hypothesis during snowmelt, *Journal of Hydrology*, Volume 219, Issues 3–4, 8 July 1999, Pages 188-205, ISSN 0022-1694, doi: 10.1016/S0022-1694(99)00059-1.

Kosugi, K., Katsura, S., Katsuyama, M., & Mizuyama, T. (2006). Water flow processes in weathered granitic bedrock and their effects on runoff generation in a small headwater catchment. *Water Resources Research*, *42*(2), n/a–n/a. doi:10.1029/2005WR004275

Loheide, S. P., & Lundquist, J. D. (2009). Snowmelt-induced diel fluxes through the hyporheic zone. *Water Resources Research*, *45*(7), W07404. doi:10.1029/2008WR007329

Lowry, C. S., Deems, J. S., Loheide II, S. P., & Lundquist, J. D. (2010). Linking snowmelt-derived fluxes and groundwater flow in a high elevation meadow system, Sierra Nevada Mountains, California. *Hydrological Processes*, *24*(20), 2821–2833. doi:10.1002/hyp.7714

Lundquist, J. D. (2005a). How snowpack heterogeneity affects diurnal streamflow timing. *Water Resources Research*, *41*(5), 1–14. doi:10.1029/2004WR003649

Lundquist, J. D. (2005b). Snow-fed streamflow timing at different basin scales: Case study of the Tuolumne River above Hetch Hetchy, Yosemite, California. *Water Resources Research*, *41*(7), 1–14. doi:10.1029/2004WR003933

Magnusson, J., Kobierska, F., Huxol, S., Hayashi, M., Jonas, T. and Kirchner, J. W. (2012), Melt water driven stream and groundwater stage fluctuations on a glacier forefield (Dammagletscher, Switzerland). *Hydrological Processes*, doi: 10.1002/hyp.9633

Martinez-Landa, L., & Carrera, J. (2005). An analysis of hydraulic conductivity scale effects in granite (Full-scale Engineered Barrier Experiment (FEBEX), Grimsel, Switzerland). *Water Resources Research*, *41*(3), n/a–n/a. doi:10.1029/2004WR003458

McGuire, K. J., & McDonnell, J. J. (2010). Hydrological connectivity of hillslopes and streams: Characteristic time scales and nonlinearities. *Water Resources Research*, *46*(10), 1–17. doi:10.1029/2010WR009341

McNamara, J. P., Chandler, D., Seyfried, M., & Achet, S. (2005). Soil moisture states, lateral flow, and streamflow generation in a semi-arid, snowmelt-driven catchment. *Hydrological Processes*, *19*(20), 4023–4038. doi:10.1002/hyp.5869

Moore, G. W., Jones, J. a., & Bond, B. J. (2011). How soil moisture mediates the influence of transpiration on streamflow at hourly to interannual scales in a forested catchment. *Hydrological Processes*, *25*(24), 3701–3710. doi:10.1002/hyp.8095

Munneke, P. K., Broeke, M. R. Van Den, Reijmer, C. H., Helsen, M. M., Boot, W., & Schneebeli, M. (2009). The role of radiation penetration in the energy budget of the snowpack at Summit, Greenland, (2005), *The Cryosphere*, 3, 155-165, doi:10.5194/tc-3-155-2009, 2009.

Newman, B. D., Wilcox, B. P. and Graham, R. C. (2004), Snowmelt-driven macropore flow and soil saturation in a semiarid forest. *Hydrological Processes*, 18: 1035–1042. doi: 10.1002/hyp.5521

Ocampo, C. J., Sivapalan, M., & Oldham, C. (2006). Hydrological connectivity of upland-riparian zones in agricultural catchments: Implications for runoff generation and nitrate transport. *Journal of Hydrology*, *331*(3-4), 643–658. doi:10.1016/j.jhydrol.2006.06.010

Penna, D., Tromp-van Meerveld, H. J., Gobbi, a., Borga, M., & Dalla Fontana, G. (2011). The influence of soil moisture on threshold runoff generation processes in an alpine headwater catchment. *Hydrology and Earth System Sciences*, *15*(3), 689–702. doi:10.5194/hess-15-689-2011

Pomeroy, J. W., Marks, D., Link, T., Ellis, C., Hardy, J., Rowlands, A. and Granger, R. (2009), The impact of coniferous forest temperature on incoming longwave radiation to melting snow. *Hydrological Processes*, 23: 2513–2525. doi: 10.1002/hyp.7325

Seyfried, M. S., Grant, L. E., Marks, D., Winstral, A., & Mcnamara, J. (2009). Simulated soil water storage effects on streamflow generation in a mountainous snowmelt environment , Idaho , USA. *Hydrological Processes*, *873*(December 2008), 858–873. doi:10.1002/hyp

Smith, M. W., Bracken, L. J., & Cox, N. J. (2010). Toward a dynamic representation of hydrological connectivity at the hillslope scale in semiarid areas. *Water Resources Research*, *46*(12), 1–18. doi:10.1029/2009WR008496

Smith, T. J., McNamara, J. P., Flores, a. N., Gribb, M. M., Aishlin, P. S., & Benner, S. G. (2011). Small soil storage capacity limits benefit of winter snowpack to upland vegetation. *Hydrological Processes*, *25*(25), 3858–3865. doi:10.1002/hyp.8340

Torres, R. (2002). A threshold condition for soil-water transport. *Hydrological Processes*, *16*(13), 2703–2706. doi:10.1002/hyp.5060

Tromp-van Meerveld, H. J., & McDonnell, J. J. (2006). Threshold relations in subsurface stormflow: 2. The fill and spill hypothesis. *Water Resources Research*, *42*(2), 1–11. doi:10.1029/2004WR003800

Wondzell, S. M., Gooseff, M. N., & McGlynn, B. L. (2010). An analysis of alternative conceptual models relating hyporheic exchange flow to diel fluctuations in discharge during baseflow recession. *Hydrological Processes*, *24*(6), 686–694. doi:10.1002/hyp.7507

Worrall, F., Howden, N. J. K., Moody, C. S., & Burt, T. P. (2013). Correction of fluvial fluxes of chemical species for diurnal variation. *Journal of Hydrology*, *481*, 1–11. doi:10.1016/j.jhydrol.2012.11.037

TABLES AND TABLE CAPTIONS:

DEPTH	Ksat (FALLING HEAD PERMEAMETER)
15 CM	1.63 meters/day
30 CM	1.50 meters/day
45 CM	1.78 meters/day
DEPTH	Ksat (GUELPH PERMEAMETER)
15 CM	0.83 meters/day
30 CM	0.93 meters/day

Table 1- Field and lab tests of hydraulic conductivity taken at multiple depths at the study hillslope.

KENDALL-MANN TREND TEST

LOCATION	TAU	P-VALUE	PASSES AT P<0.1?
WELL 1	-0.037	0.846	NO
WELL 2	-0.042	0.762	NO
WELL 3	0.36	0.058	YES
WELL 4	-0.316	0.0043	YES
WELL 5	-0.141	0.675	NO

LINEAR REGRESSION TREND TEST

LOCATION	TAU	P-VALUE	PASSES AT P<0.1?
WELL 1	-0.310	0.76	NO
WELL 2	-1.432	0.163	NO
WELL 3	-0.103	0.919	NO
WELL 4	-5.719	1.38×10^{-6}	YES
WELL 5	-1.671	0.139	NO

Table 2- The Kendall-Mann statistical trend test yields statistically significant results for wells 3 and 4 at a P<0.1. Only well 4 has a statistically significant linearly decreasing trend according to a linear regression model.

FIGURES AND FIGURE CAPTIONS:

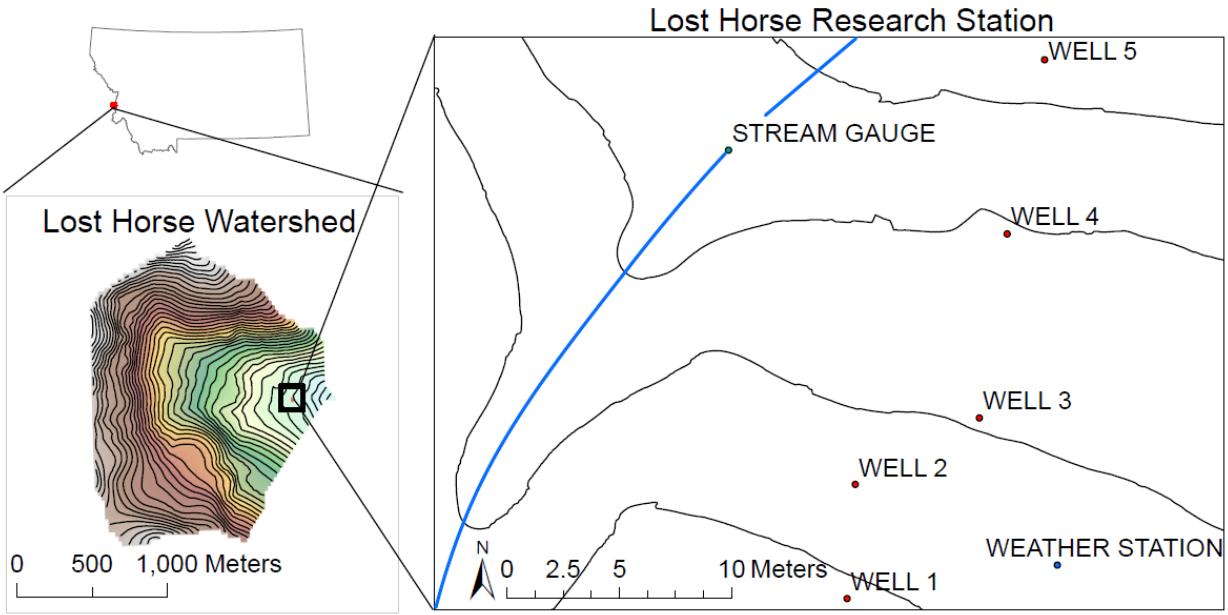

Figure 1- Inset maps showing the location of the research watershed in western Montana, the topography of the research watershed, and the instrumentation design for this study. The study area is located in a clearing and surrounded by trees.

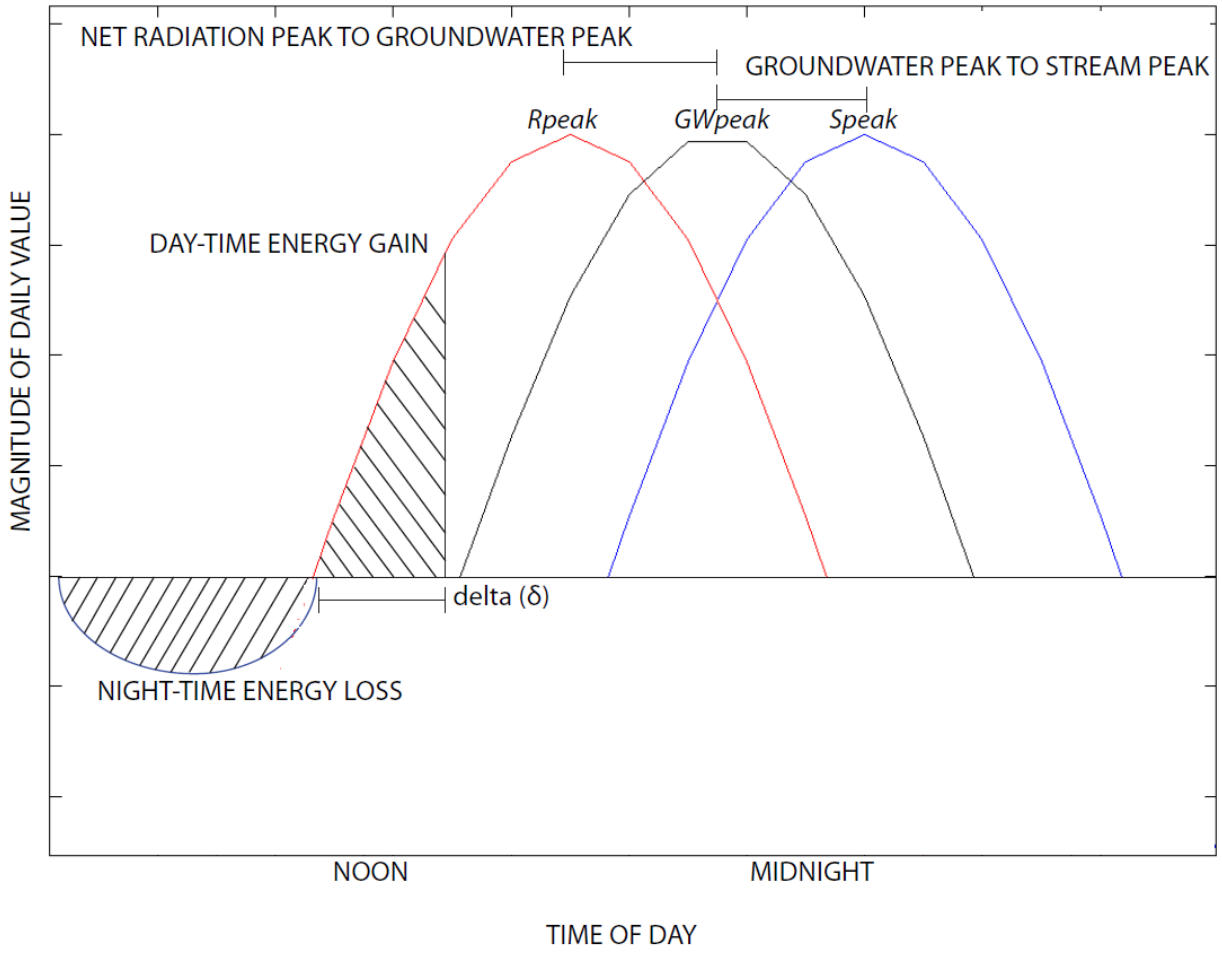

Figure 2- Conceptual diagram showing daily cycles of net radiation, well response, and stream stage. Daily peaks in shallow groundwater levels consistently lag peaks in net radiation, while daily peaks in stream stage consistently lag that of well response. Night-time energy loss is the sum of all radiative energy lost from the snowpack during the night. Day-time energy gain is a sum of all radiative energy gained during the early portion of the day needed to meet or exceed night-time energy loss. Delta (δ) is a measure of the time needed for day-time radiative energy gain to meet or exceed night-time radiative energy loss. R_{peak}, GW_{peak}, and S_{peak} are measurements of the timing of the daily maxima in net radiation, groundwater levels, and stream stage, respectively. Differencing R_{peak} and GW_{peak} provides a measure of the travel time of the daily melt signal from the top of the snowpack to groundwater stored in a hillslope. Differencing GW_{peak} and S_{peak} provides a measure of the travel time of the daily melt signal from groundwater stored in a hillslope to the local stream system.

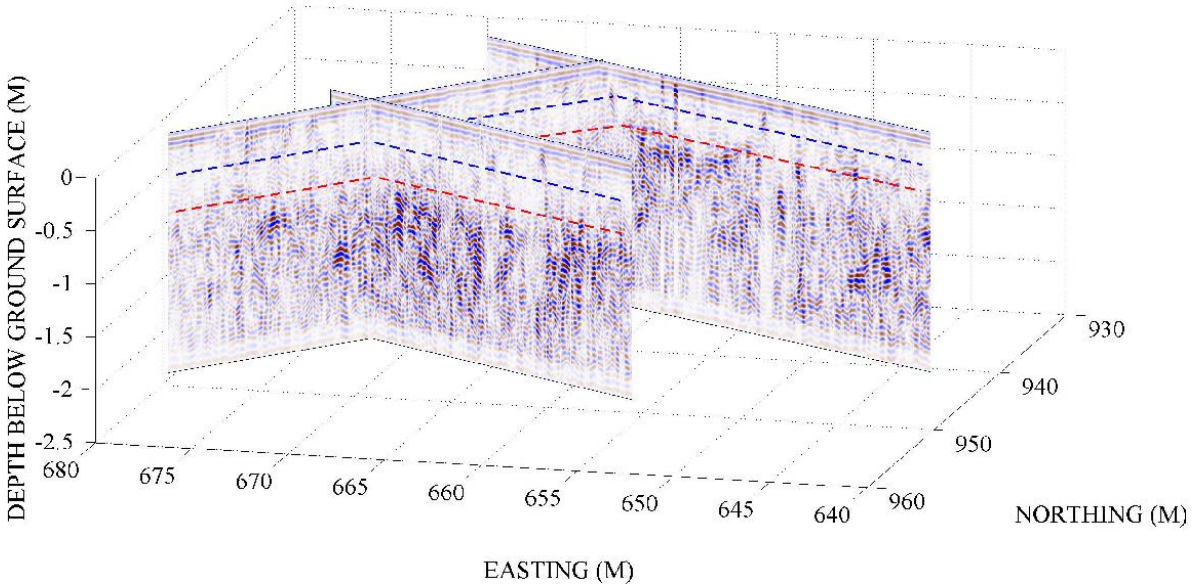

Figure 3- Fence diagram of three select ground penetrating radar transects used to characterize the Lost Horse Canyon research site. The dashed blue line indicates the point of refusal to which hand-tools can reach. The red line indicates the location of un-weathered granite bedrock.

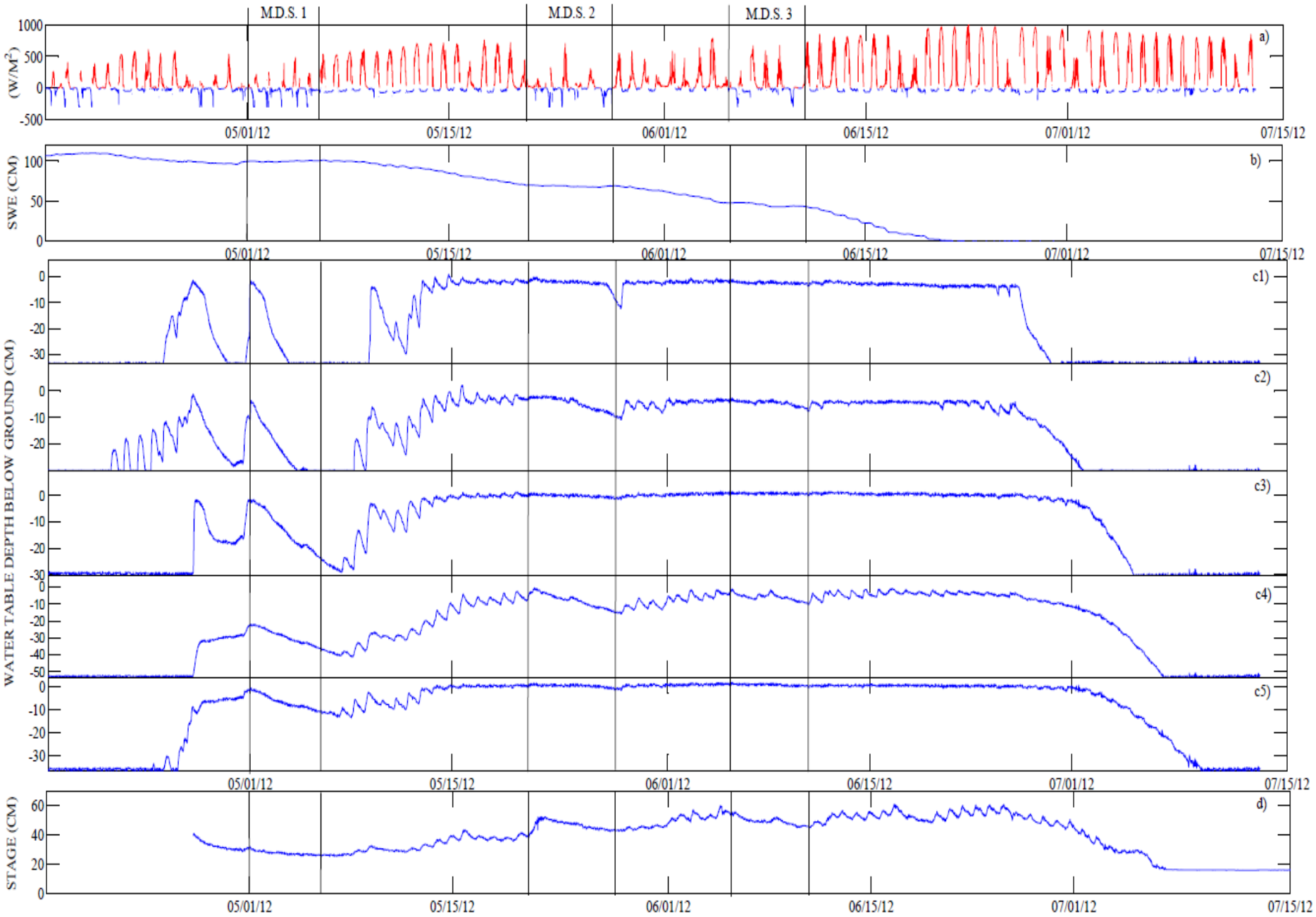
M.D.S. 1
M.D.S. 2
M.D.S. 3
(W/M²)
a)
SWE (CM)
b)
WATER TABLE DEPTH BELOW GROUND (CM)
c1)
c2)
c3)
c4)
c5)
STAGE (CM)
d)
05/01/12
05/15/12
06/01/12
06/15/12
07/01/12
07/15/12

Figure 4- Net radiation (a), snow water equivalent (b), groundwater level below the surface in wells 1-5 (c1-c5), and stream stage (d) during the spring melt. Fluctuations in net radiation represent the energy fluxes between the snowpack and atmosphere. SWE decreases during melt events, but remains constant during multi-day storms. Three major multi-day storms occur during the spring melt, and are bracketed with solid vertical lines and labeled M.D.S. 1-3. Hillslope response to snowmelt can be seen in five wells. All wells are highly variable early in the melt season, remain fully saturated during the spring melt, and draw down gradually at the end of the melt season. Stream stage varies in response to changes in the water table.

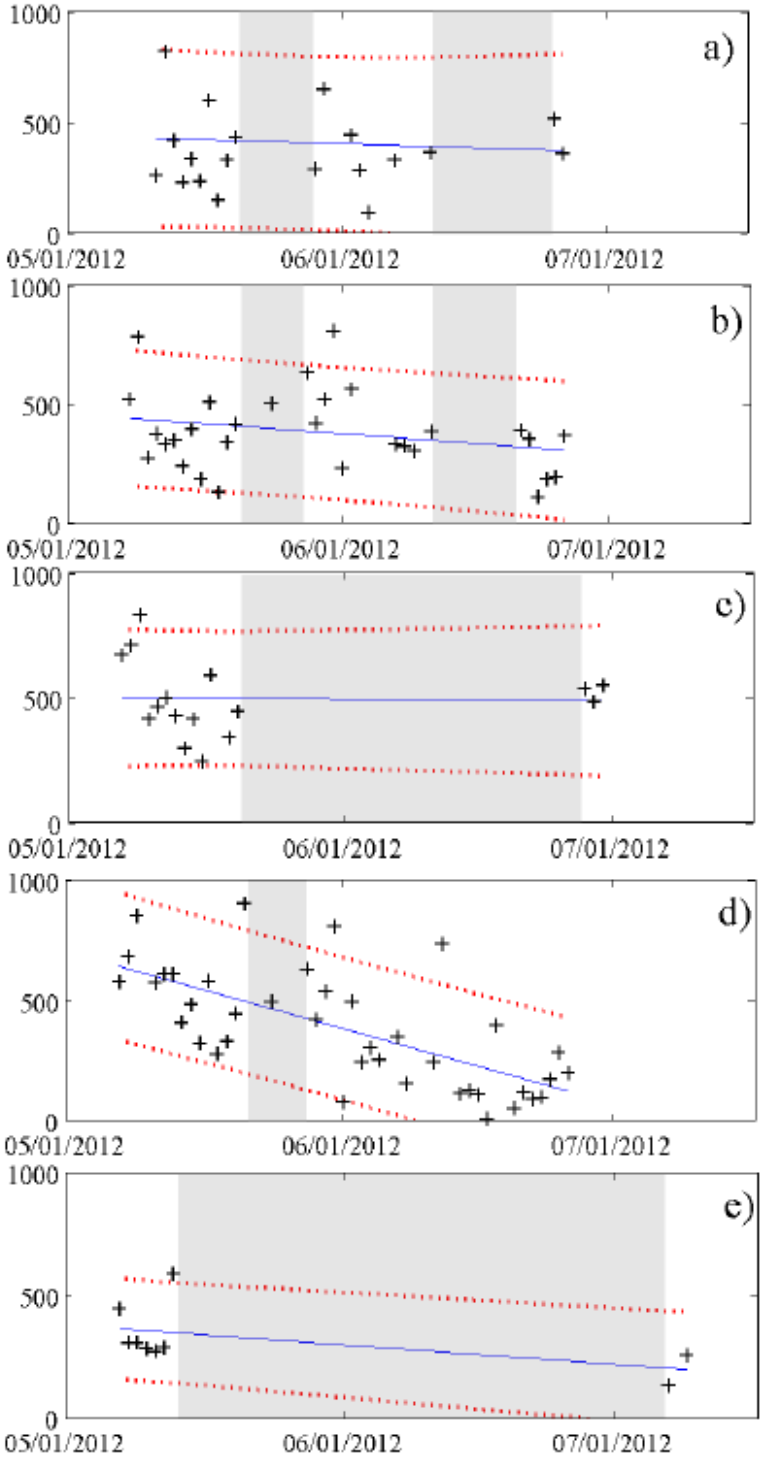

Figure 5- Time from daily peak in net radiation to daily peaks in wells 1-5 (a-e) versus day of the year. The seasonal trend in all wells is negative, varying from -0.22 min/day (well 3) to -10.32 min/day (well 4). 90% confidence bounds in red show the uncertainty of the linear trend shown in blue. Times of full well saturation are indicated with grey shading. During these times, there is no change in diurnal groundwater level and any additional snowmelt translates into overland flow.

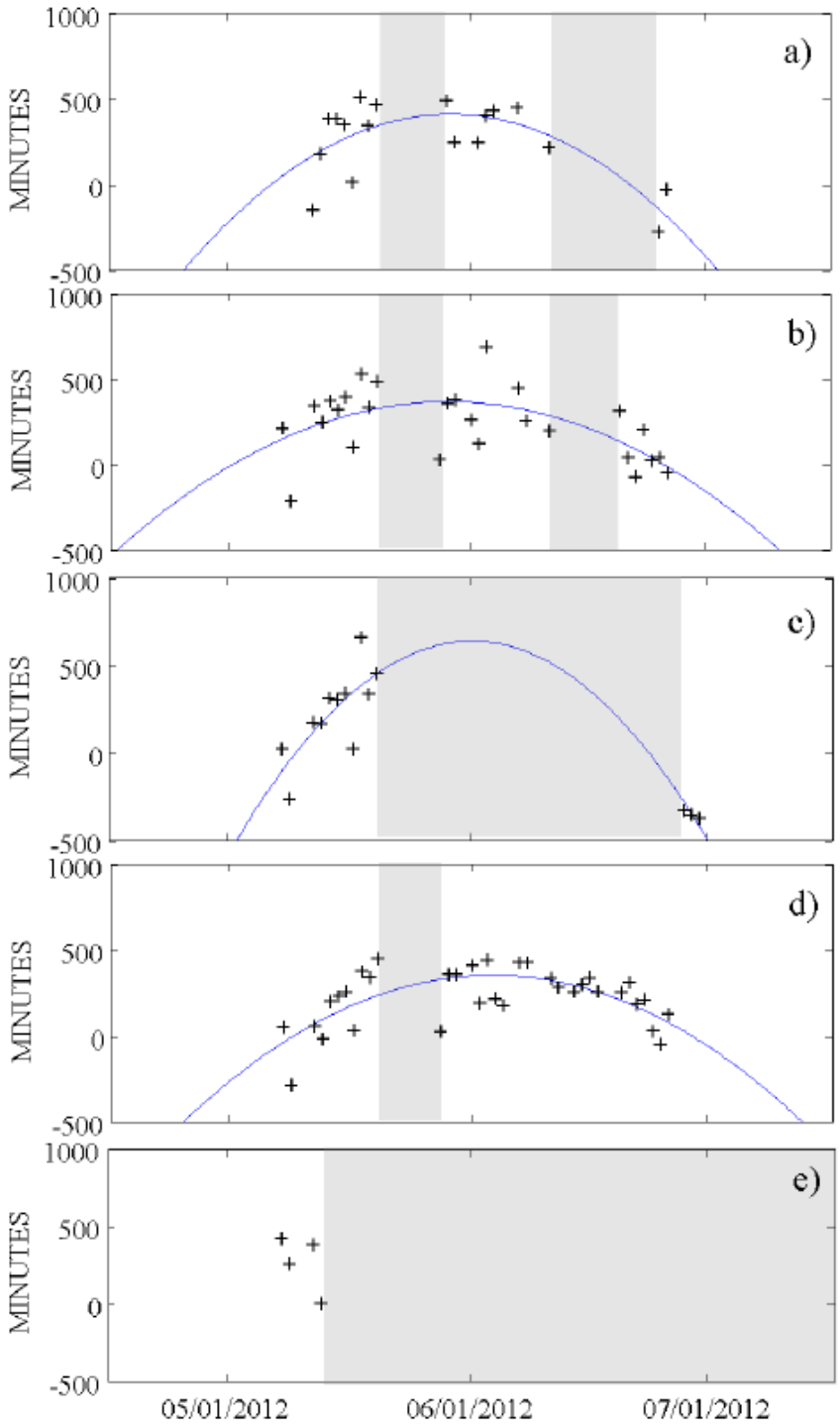

Figure 6- Time from daily peaks in wells 1-5 and daily peak in stream stage (a-e) versus day of the year. Wells one to four are fit with a quadratic trend line, with a small signal travel time early in the melt season, a large signal travel time in the middle of the melt season, and a small signal travel time late in the melt season. Too few observations exist to fit well five with a meaningful trend. Times of full well saturation are indicated with grey shading. During these times, there is no change in diurnal groundwater level and any additional snowmelt translates into overland flow.

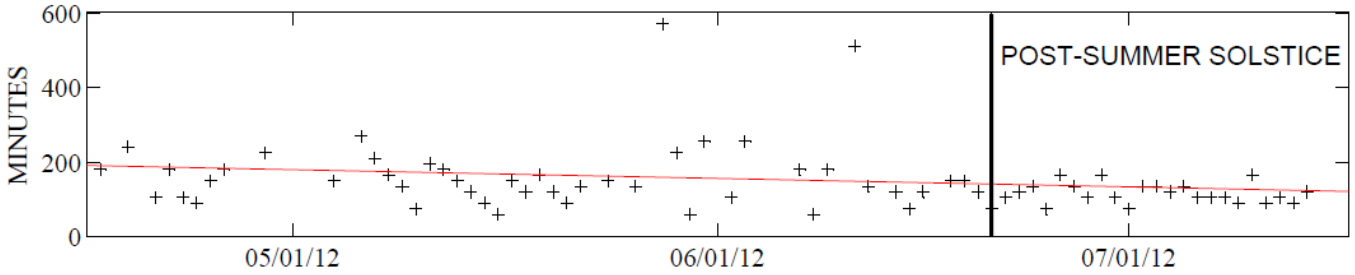

Figure 7- Daily replenishing time (δ) versus day of the year. Each marker indicates the duration before positive radiative inputs during the day exceed nightly outputs during the previous night, for each day of the melt season. This calculation provides an estimate of the amount of time before the snowpack surface is re-melted and the entire snowpack is returned to an output phase. As both days and nights become warmer, and nights become shorter until the summer solstice, the time required to bring the snowpack to its daily output phase decreases. The summer solstice is highlighted with a vertical line.

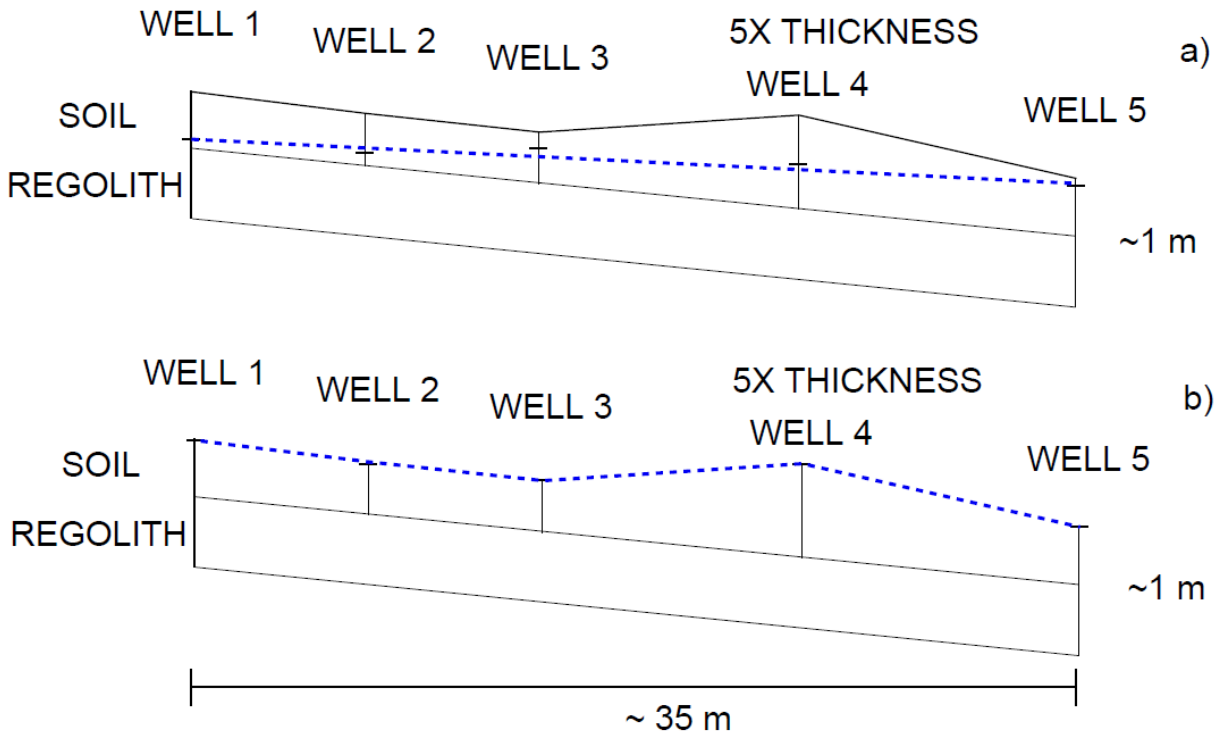

Figure 8- Conceptual diagram of hillslope dynamics during the spring melt, 5x exaggeration of hillslope thickness. During portions of the year transient drawdowns reduce the height of the water table in uphill wells more than downhill wells, forming a saturated wedge of water (panel a). During most portions of the year, the entire hillslope is saturated and the water table mirrors the land surface. During these times, daily additions of meltwater translate rapidly to overland flow.